(16) M. Arpin and C. Strazielle, *Polymer*, 18, 591 (1977).
(17) V. N. Tsvetkov and I. N. Shtennikova, *Macromolecules*, 11, 306 (1978).
(18) Yoon and Flory[13] derived the scaling ratio m from reduced moments of the "displacement vector" $\rho = \mathbf{r} - \mathbf{a}$, instead of from the reduced moments of the chain vector $\mathbf{r}$ itself, as in eq 35. In as much as the reduced displacement vector defined by $\rho = \langle\rho\rho^{T}\rangle^{-1/2}\rho$ converges to the reduced chain vector $\tilde{\mathbf{r}}$ in the limit $1/n \rightarrow 0$, these alternative procedures must lead to the same value of the scaling ratio m.

Unperturbed Dimensions of Amylose in Binary Water/Dimethyl Sulfoxide Mixtures‡

Robert C. Jordan and David A. Brant*

Department of Chemistry, University of California, Irvine, California 92717.
Received December 20, 1979

ABSTRACT: The unperturbed dimensions of amylose have been determined in the mixed solvent water/dimethyl sulfoxide (Me_2SO) over the range of Me_2SO volume fraction (Φ_{Me_2SO}) from 0.30 to 0.90. The molecular weight, second virial coefficient, and mean square radius of gyration were measured for 11 different values of Φ_{Me_2SO} by light scattering. Intrinsic viscosities have been determined in the same solvent mixtures. The excluded volume expansion factor was evaluated from the observed molecular weights, virial coefficients, and polymer chain dimensions with the modified Flory–Krigbaum–Orofino theory and the Yamakawa–Tanaka theory and used in conjunction with chain dimensions from both light scattering and intrinsic viscosity to calculate the unperturbed dimensions. In the mixed solvent the unperturbed mean-square end-to-end distance declines from its value in water to about 80% of this value at $\Phi_{Me_2SO} = 0.60$; further variation for $\Phi_{Me_2SO} > 0.60$ cannot be ascertained with confidence. The observed effect of specific solvation on the unperturbed dimensions is discussed in terms of changes in the preferred conformational isomers for rotations about the chemical bonds of the glycosidic linkage.

The dilute solution behavior of most common polysaccharides has now been analyzed in terms of more or less realistic molecular models, and a framework for rationalizing solution properties in terms of molecular structure and conformation has been established.[1,2] No member of the class has received more attention than amylose, the linear α-1,4-glucan component of starch,[3] and a good understanding of the molecular basis for its aqueous solution characteristics has emerged.[4-6] As yet no detailed model has been presented for the influence of specific solvation effects on the unperturbed dimensions of amylose or any other polysaccharide, although it is widely recognized that the polar character of these polymers and their common solvents makes likely an important influence of strong solvation on the conformational energy surface of the chain.[7] It is as part of an effort to understand the role of specific solvation in polysaccharide solution behavior that the studies reported here were undertaken.

Figure 1 shows a conventional conformational energy map[7,8] for the dimeric amylose chain segment "maltose". The maltose unit is shown as an inset on the map, and the glycosidic linkage torsion angles φ and ψ are defined; conventions for the zero and positive sense of rotation are given elsewhere.[2,7] The map shown, although correct for *aqueous* amylose in its major features, does not reflect any explicit accounting of solvation effects and has not been refined to conform to any measured solution characteristics of amylose.[2,7]

Amylose has been studied extensively in H_2O and dimethyl sulfoxide (Me_2SO) solution, and its properties in the binary solvent H_2O/Me_2SO have also been investigated. Metastable solutions of amylose in water can be prepared, from which amylose in the B-crystalline modification precipitates in a process known as retrogradation.[9-13] The rate of retrogradation displays a strong dependence on mean molecular weight and molecular weight distribution.[9,12] In favorable cases it has therefore been possible to investigate the solution characteristics of amylose in water and in aqueous salt solutions. It is widely believed that aqueous 0.33 M KCl is a Θ solvent for the polymer[3,14] in which the characteristic ratio $C_\infty \equiv \langle r^2\rangle_0/xL^2 \simeq 5$, where $\langle r^2\rangle_0$ is the mean-square unperturbed end-to-end distance, x is the degree of polymerization, and L is the length of the virtual bond (4.25 Å)[8] connecting successive glycosidic oxygens. Molecular models for aqueous amylosic chains are well developed and suggest that the dissolved polymer is a mobile random coil with a tortuous backbone trajectory that nevertheless displays at any instant considerable irregular short-range helical structure.[6]

In contrast to water, Me_2SO is a good solvent for amylose, and the intrinsic viscosity, radius of gyration, and second virial coefficient are considerably larger for a given amylose sample in Me_2SO than in H_2O solution.[11,15-19] Fujii et al.[19] conclude from studies of the chain length dependence of the intrinsic viscosity, radius of gyration, virial coefficient, and sedimentation coefficient of amylose fractions that the molecular conformation of the polymer in Me_2SO is stiff and "predominantly helical, in contrast to that of the same polymer in aqueous solutions of simple electrolyte". Proton magnetic resonance (^1H NMR) and infrared spectroscopic studies of amylose and model compounds[20] reveal the presence in Me_2SO solution of an interresidue hydrogen bond between hydroxyls OH(2) and OH(3′). St. Jacques et al. infer from further ^1H NMR studies[21] that OH(3′) is the proton donor in this interaction and conclude that the favored conformations of the glycosidic linkage torsion angles φ and ψ (see Figure 1) are such as to confer on the chain "substantial right-handed helical character in this solvent". Maltose conformations with positive values of φ and ψ in the vicinity of the position marked Z on the energy map in Figure 1 are implied by this proposal.[21]

Molecular models for aqueous amylosic chains, on the other hand, are unanimous in their implication that the residual helical character in this medium has predominantly left chirality.[4-6,22,23] The lowest energy conformation in Figure 1, for example, is in the field of left helical states

‡ Dedicated to Professor Paul J. Flory on the occasion of his 70th birthday.

0024-9297/80/2213-0491$01.00/0

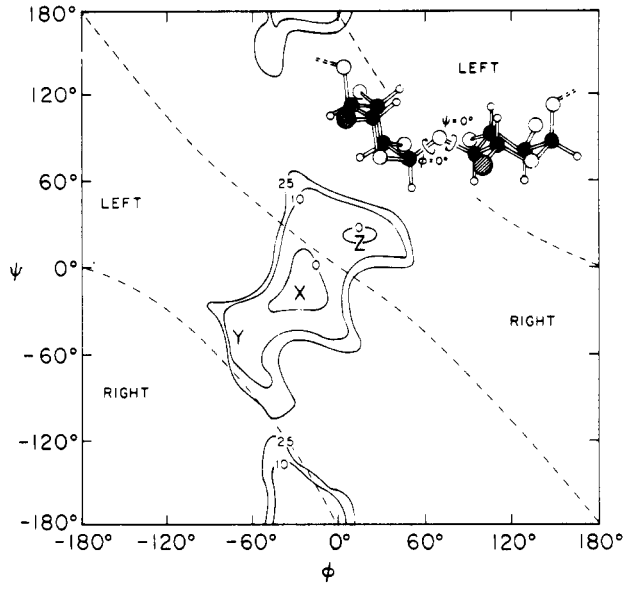

Figure 1. Maltose conformational energy map. Solid contours give energies in kcal/mol. Dashed contours divide the conformation space into domains of right and left helix chirality. The diagonal dashed contour marks the locus of conformations which, if repeated in sequence, generate helices of vanishing pitch. Other features of the figure are described in the text.

at the position marked X where φ and ψ are both negative. It must be remarked, however, that the principal domain of low energy in the φ,ψ conformation space of the maltose unit in Figure 1 has a rather flat bottom that allows for the occurrence of conformations with both left and right helical chirality with approximately equal probability.[2,5,7] Moreover, it is important to recognize that the energy contours and the boundaries in φ,ψ space of the fields of left and right helical character depend significantly on the structural geometries chosen for the residue and the linkage.[8] Consequently, differing conclusions about the chirality of the residual helicity in dissolved amylosic chains can result from rather small differences in choice of conformational energy functions and skeletal geometry and may not be particularly significant. Nevertheless, Rees and Thom,[23] on the basis of chiroptical measurements on maltose in H_2O and Me_2SO solution, provide additional support for the possibility that the conformational preference of maltose in Me_2SO solution is shifted, relative to the least energetic conformers in H_2O, toward conformations characterized by more positive values of both φ and ψ. Thus, conformations with left helical chirality in the vicinity of the position marked Y in Figure 1 are believed by Rees and Thom[23] to be preferred by maltose in aqueous solution, whereas the preference is thought to shift in Me_2SO toward conformers closer to position X.

In mixtures of H_2O and Me_2SO the intrinsic viscosity, $[\eta]$, of amylose increases by a factor of about three in passing from pure H_2O to pure Me_2SO.[24] A plot of $[\eta]$ vs. volume fraction of Me_2SO (Φ_{Me_2SO}) lies below the linear curve connecting the values of $[\eta]$ in pure H_2O and pure Me_2SO[24] as is characteristic of the intrinsic viscosities of polymers dissolved in binary solvent mixtures formed with a negative excess free energy of mixing.[25] Unlike many other reported examples of $[\eta]$ vs. binary solvent composition,[25-27] the plot of $[\eta]$ vs. Φ_{Me_2SO} for amylose in H_2O/Me_2SO mixtures has regions of both positive and negative curvature. A minimum appears in the curve near $\Phi_{Me_2SO} = 0.25$, but the Mark–Houwink exponent a is larger in this solvent mixture than in 0.5 M aqueous KCl.[24] This suggests[24] that the unperturbed dimensions of amylose may be smaller in this binary solvent mixture than they are in 0.5 M aqueous KCl, which closely approximates a Θ solvent for the polymer.

Dintzis and Tobin[28] have measured the specific rotation $[\alpha]$ of amylose, amylopectin, glycogen, cyclohexaamylose, β-methyl maltoside, sucrose, and dextran as a function of the binary solvent composition in H_2O/Me_2SO mixtures. The first three species, all of which contain high polymeric sequences of α-(1,4)-glucan chain, show a dependence of $[\alpha]$ on Φ_{Me_2SO} that may be approximated as two straight line segments of different slope which intersect near $\Phi_{Me_2SO} = 0.66$. None of the other species studied, including the two oligomeric α-(1,4)-glucans, display this discontinuity in slope. Dintzis and Tobin[28] attributed the discontinuity observed for amylose and the two branched high polymeric α-(1,4)-glucans to a change in "the distribution of preferred rotation angles between maltose units". They called attention to the possible importance of the well-known 2:1 (H_2O:Me_2SO) complex, the stoichiometry of which is satisfied exactly at $\Phi_{Me_2SO} = 0.66$ where the slope discontinuity occurs.[29,30] If the H_2O/Me_2SO interaction is stronger than that of either solvent component with the polymer as proposed by Cowie,[24] then in the limiting case it is possible to imagine that the polymer is solvated only by H_2O when $\Phi_{Me_2SO} < 0.66$ and only by Me_2SO when $\Phi_{Me_2SO} > 0.66$.[28] Recent gel permeation chromatography (GPC) measurements[31] confirm that amylose and other glucans in H_2O/Me_2SO mixtures are preferentially solvated (relative to the bulk binary solvent composition) by H_2O for $\Phi_{Me_2SO} < 0.66$ and by Me_2SO for $\Phi_{Me_2SO} > 0.66$, but the absolute composition of the solvation sheath is not accessible from the GPC experiment. It is interesting to remark, however, that the measured values of $[\alpha]$ for amylose in mixtures with $\Phi_{Me_2SO} > 0.66$ are constant,[28] and this is at least consistent with a constant composition of the solvation sheath throughout this range of solvent mixtures.

The ^{13}C NMR resonances of all carbons in amylose and several maltodextrins have been assigned and reported as functions of Φ_{Me_2SO} in binary H_2O/Me_2SO solvent mixtures.[32] For maltose the chemical shifts of all of the carbons move linearly upfield with Φ_{Me_2SO} except for those of the C(4) involved in the glycosidic linkage which move linearly downfield. The signal for the C(1) involved in the glycosidic linkage is a singlet in pure H_2O and pure Me_2SO but is split into a doublet for mixtures in the range $0.25 \leq \Phi_{Me_2SO} \leq 0.75$. For amylose the ^{13}C chemical shifts vary with Φ_{Me_2SO} as do those for maltose, except that the dependence is no longer linear and the chemical shift for C(4) passes through a maximum. There is no evidence in the ^{13}C NMR results that the properties of the polymer do not vary continuously with solvent composition, or that any particular H_2O/Me_2SO mixture has a special significance.

The foregoing review of the properties of amylose and maltose dissolved in H_2O, Me_2SO, and H_2O/Me_2SO mixtures suggests strongly that changes in the solution properties of amylose with solvent composition result at least in part from corresponding variations in the short range interactions which influence the conformational preferences of the linkage torsions φ,ψ. Expressed in terms of the energy surface for first neighbor interactions in Figure 1, this means that the locations of energy contours in the low-energy domain of the map must shift as the map is refined to be consistent with the observed unperturbed polymer properties in binary H_2O/Me_2SO solvents of different compositions. Although it is common to assume that the properties of unperturbed polysaccharides can be represented adequately in terms of the energy surfaces of

independent dimeric subunits,[7,33] one must also acknowledge that considerations of longer range interdependent energy contributions may need to be invoked to explain fully the effects of specific solvation on the properties of the unperturbed chain.[6] The present paper reports an effort to determine the mean square unperturbed coil dimensions of amylose as a function of the composition of the binary solvent H_2O/Me_2SO for eventual use in making refinements of the energy surface of Figure 1 to reflect the role of specific solvation on the conformational preferences of the α-(1,4)-glucan linkage torsion angles.

Experimental Section

Preparation of Polymer Solutions. A purified polydisperse potato amylose sample of high iodine binding capacity (NRRC 5658:21), prepared according to Schoch,[34] was provided by Dr. R. J. Dimler of the USDA Northern Regional Research Center, Peoria. Solvents were distilled H_2O from a central distillation unit and analytical grade Me_2SO (Mallinkrodt, "AR"). The polymer was dissolved by weighing accurately ca. 0.4 g of amylose, vacuum dried at 65 °C, into a known volume (ca. 8 mL) of Me_2SO. This solution was stirred at room temperature for 10–12 h and diluted volumetrically to ca. 1% amylose with an H_2O/Me_2SO mixture chosen to produce the desired mixed solvent composition. (Volume fractions Φ_{Me_2SO} are reported on the basis of the volumes of the pure solvents.) The 1% stock solutions were centrifuged at 20 000 rpm (Beckman Spinco Model L, Type 30 head) for ca. 1 h. Trace amounts of sedimented material were ignored in calculating the polymer concentration. Approximately 35 mL of the centrifuged stock solution were dialyzed at constant temperature for at least 30 h in a stirred constant-volume cell against a large excess of binary solvent of the same Φ_{Me_2SO}; the Schleicher and Schuell membranes (Type RC52) were preconditioned to the solvent mixture. Solutions for light scattering, differential refractometry, and viscometry were prepared by volumetric dilution of the dialyzed stock solution with dialyzate to fulfill the requirements[35] for convenient interpretation of the light-scattering experiments. In experiments conducted at temperatures other than 25 °C, effects of thermal expansion on the polymer concentration were taken into account by using measured solvent densities at the temperatures in question. Measurements were restricted to the range of binary solvents $0.30 \leq \Phi_{Me_2SO} \leq 0.90$. The behavior of amylose in pure H_2O and pure Me_2SO is well documented in work already cited, and amylose dissolved in H_2O/Me_2SO mixtures with $\Phi_{Me_2SO} < 0.30$ was subject to retrogradation during the required dialysis.

Light-Scattering Measurements. Light-scattering measurements were made with a SOFICA Model 42000 instrument by using unpolarized incident light with wavelength $\lambda = 436$ nm and with a 436-nm filter in the scattered light train. Details of the experiments, including temperature control, scattering cells, and clarification of solutions by centrifugation in the floating cells,[36] were very similar to the description given earlier.[14] Filtrations were done by using 5μ Teflon filters (Millipore Mitex), and the floated cells were centrifuged for 45–60 min at 18 000 rpm in a Spinco Type 25.1 rotor. Satisfactory optical performance of the instrument and cells was verified by comparing the measured angular dependence of the scattering of pure benzene with literature reports.[37,38] The optical constant K of the light-scattering equations is defined as it was earlier;[14] the refractive index increment which enters K was measured at constant chemical potential of the binary solvent components[35] as described below with amylose concentrations expressed in grams per milliliter. Changes with temperature of the Rayleigh ratio of benzene and the refractive indices of benzene and mixed solvent were taken into account as required.

Scattering intensities were measured for each solvent composition over the angle range $30 \leq \theta \leq 150°$ on six polymer solutions with concentrations c_2 in the range 0.001–0.004 g/mL. Scattering from mixed solvents, needed to obtain the excess scattering $i(\theta)$ due to dissolved polymer, was observed to be unexpectedly large at angles below 60° in the solvent composition range $0.5 \leq \Phi_{Me_2SO} \leq 0.7$, and this effect was more pronounced in the dialyzates than in undialyzed solvent of the same composition. Consequently, data from undialyzed mixed solvents were used in this range of Φ_{Me_2SO} to obtain $i(\theta)$. In no case did the binary solvent scattering exceed 10% of the scattering from the most dilute polymer solutions at the same angle and solvent composition.

The data were plotted by using Zimm's method[39,40] as $Kc_2/\alpha i(\theta)$ vs. $\sin^2(\theta/2) + kc_2$, where α is defined elsewhere[14] and k is a constant chosen arbitrarily to produce a plot suitable for convenient extrapolation to vanishing c_2 and θ. It was assumed that this plot is related to the weight average molecular weight, M_w, the mean-square z-average radius of gyration, $\langle s^2 \rangle_z$, and the light-scattering second virial coefficient, A_2', of the polymer by eq 1,[39,40] where n is the refractive index of the mixed solvent.[41,42]

$$\frac{Kc_2}{\alpha i(\theta)} = \frac{1}{M_w}\left[1 + \frac{16\pi^2\langle s^2\rangle_z}{3(\lambda/n)^2}\sin^2(\theta/2)\right] + 2k^{-1}A_2'c_2 \quad (1)$$

The use of eq 1 in the present case is justified by arguments presented below.

The angular dependence of $Kc_2/\alpha i(\theta)$ showed significant negative curvature in all Zimm plots in the range $30 \leq \theta \leq 90°$ but was consistently linear for $\theta > 90°$ (see, e.g., Figure 4). Values of M_w and $\langle s^2 \rangle_z$ obtained by using eq 1 at vanishing c_2 from the limiting angular dependence at small θ were unrealistically large; considerations of the high angle data only (defined as $\theta > 90°$) yielded reasonable and consistent values for M_w and $\langle s^2 \rangle_z$. Moreover, the concentration dependence of $Kc_2/\alpha i(\theta)$ at high angle consistently yielded linear, parallel lines (Figure 4) which were assumed to reflect the true value of A_2' normally obtained from the concentration dependence at $\theta = 0°$. Therefore in every case M_w and $\langle s^2 \rangle_z$ were calculated by using eq 1 from the angular dependence of $Kc_2/\alpha i(\theta)$ at vanishing c_2 in the range $100 \leq \theta \leq 150°$, while A_2' was calculated as $(k/2)$ times the slope of the concentration dependence of $Kc_2/\alpha i(\theta)$ at $\theta = 100°$. Note that negative values of k were normally preferred as in Figure 4.[43] We attribute the strong angular dependence of scattering at low angles to the presence of a small weight fraction of very high molecular weight species in the amylose solutions, a situation frequently reported for amylose[44] and other polysaccharides.[45-47] A justification for restricting attention to the high angle data is presented in the Discussion.

Refractive Increment Measurements. The refractive index increment $(\partial n/\partial c_2)_\mu$ at $\lambda = 436$ nm was measured at constant T and constant chemical potential of H_2O and Me_2SO[35] by using a Brice-Phoenix differential refractometer. The light-scattering solutions were used following the scattering experiment to measure the refractive increment at the corresponding temperatures. It was essential to use a refractometer cell with stoppered compartments to obtain reliable results. The refractive increment was found to be independent of c_2 in the range 0.002–0.0035 g/mL within the limits of experimental error, and results presented below represent an average of measurements on at least three solutions of different polymer concentration.

Intrinsic Viscosity Measurements. Flow times, t_0 and t, were measured on solvent (dialyzate) and amylose solutions, respectively, following their use in light-scattering and differential refractometry measurements. A Cannon-Ubbelohde Size 75 dilution viscometer was employed, except that a Size 100 was used for $\Phi_{Me_2SO} > 0.70$ and for the 15 °C measurement in the temperature dependence work at $\Phi_{Me_2SO} = 0.45$. The temperature was controlled to ±0.01 °C except for measurements at 15 and 45 °C where variations of ±0.05 °C were tolerated. A mean deviation of less than ±0.1 s from the mean of three successive flow times was demanded. Dialyzate flow times ranged from 160 to 380 s, and relative viscosities ($\eta_r = t/t_0$) were confined to the range 1.04–1.68. Consequently, no kinetic energy corrections were required.[48] Shear dependence of the measurements was also negligible.[17] Intrinsic viscosities $[\eta]$ were taken as the value of $(\eta_r - 1)/c_2$ at the limit of vanishing c_2.

Experimental Results

Viscometry. The results of measurements of $[\eta]$ as a function of Φ_{Me_2SO} at 25 °C and as a function of temperature at $\Phi_{Me_2SO} = 0.45$ are given in column 2 of Table I. These data are plotted in Figure 2. Uncertainties associated with the values of $[\eta]$ in Table I reflect the reproducibility of the measured flow times; they are not dis-

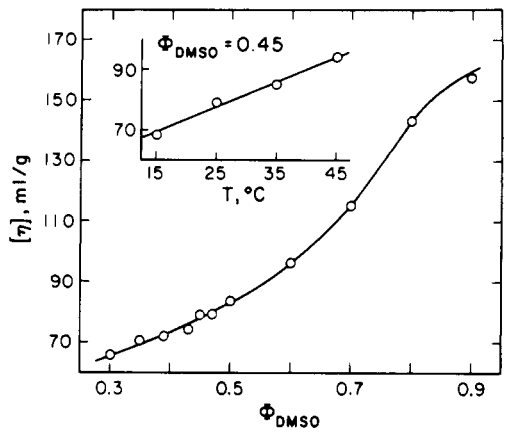

Figure 2. The intrinsic viscosity of amylose, $[\eta]$, plotted against the volume fraction of Me_2SO, Φ_{Me_2SO}, at 25 °C. The inset shows $[\eta]$ as a function of temperature at $\Phi_{Me_2SO} = 0.45$.

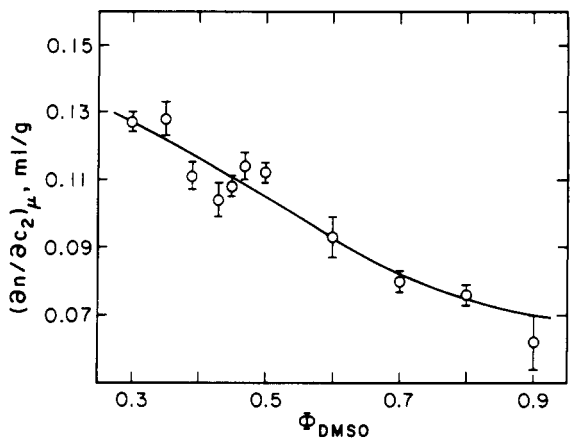

Figure 3. A plot vs. Φ_{Me_2SO} of the differential refractive index increment of amylose, $(\partial n/\partial c_2)_\mu$, measured at 25 °C and constant chemical potential of all membrane diffusible components.

cernible on the scale of Figure 2 and are therefore omitted in the figure.

Differential Refractometry. The measured values of $(\partial n/\partial c_2)_\mu$ are given in column 3 of Table I and in Figure 3 as functions of Φ_{Me_2SO} at 25 °C and, in Table I only, as a function of temperature at $\Phi_{Me_2SO} = 0.45$. Estimated experimental uncertainties shown in Table I and Figure 3 arise from consideration of the range of measured $(\partial n/\partial c_2)\mu$ values obtained on three or four solutions of different polymer concentration. The values of $(\partial n/\partial c_2)_\mu$ obtained at various temperatures for $\Phi_{Me_2SO} = 0.45$ show an unusual temperature dependence,[49] and the light-scattering results for M_w calculated by using these $(\partial n/\partial c_2)_\mu$ values vary strongly with temperature. Hence, we believe some of these data to be burdened by serious systematic error, and experimental uncertainties have been assigned only for the seemingly satisfactory results at 25 °C.

The smooth curve in Figure 3 was fitted by visual inspection to the measured $(\partial n/\partial c_2)_\mu$ values, taking into account the known refractive increments for amylose in Me_2SO[15] and H_2O (0.33 M KCl),[50] i.e., at $\Phi_{Me_2SO} = 1$ and 0. The mean deviation of experimental points from this line is ±3.6%. This scatter may be due in part to failure to attain complete dialysis equilibrium in all cases. Some calculations below are made by using "smoothed" refractive increment values $(\partial n/\partial c_2)_\mu$* taken from the smooth curve. These are given in column 4 of Table I, and their ratios to the measured values are in column 5. An experimental uncertainty of ±3.6% was attributed to all values of $(\partial n/\partial c_2)_\mu$* in Table I.

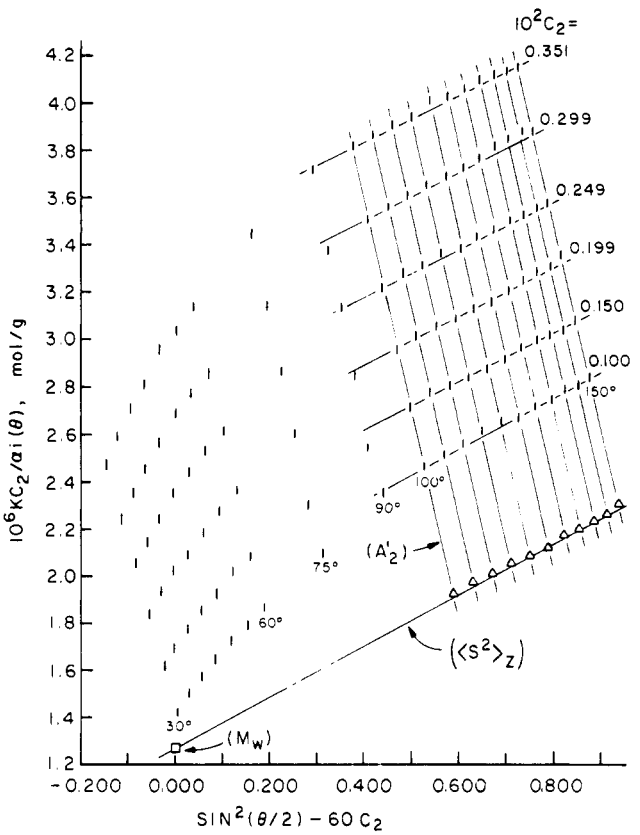

Figure 4. The Zimm plot constructed from light-scattering data on amylose at $\Phi_{Me_2SO} = 0.90$ and 25 °C. Straight lines are drawn through the data at each concentration c_2 (g/mL) and angle θ (degrees) for $100 \leq \theta \leq 150°$. Triangles denote data extrapolated to $c_2 = 0$. Experimental values of $\langle s^2\rangle_z$, A_2', and M_w were obtained from the lines and intercepts of the plot as indicated.

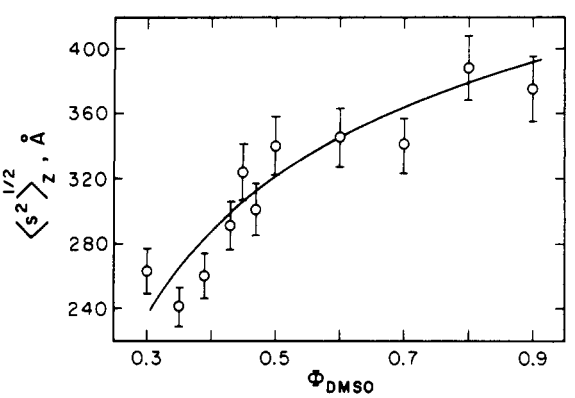

Figure 5. The light-scattering root-mean-square radius of gyration of amylose, $\langle s^2\rangle_z^{1/2}$, as a function of Φ_{Me_2SO} at 25 °C.

Light Scattering. Values of M_w, A_2', and $\langle s^2\rangle_z^{1/2}$ measured as a function of Φ_{Me_2SO} and temperature are presented in columns 6, 7, and 8 of Table I, respectively. Molecular weights M_w* and virial coefficients A_2'*, calculated by using $(\partial n/\partial c_2)_\mu$* instead of $(\partial n/\partial c_2)_\mu$, are given, respectively, in columns 9 and 10 of Table I. The mean values of M_w and M_w*, which we denote, respectively, by $\bar{M}_w$ and $\bar{M}_w$*, are (6.06 ± 0.93) × 10^5 and (5.88 ± 0.62) × 10^5, where only the data at 25 °C are included and the uncertainties indicated are the standard deviations. The Zimm plot shown for $\Phi_{Me_2SO} = 0.90$ in Figure 4 is typical of those obtained in all of the experiments except for the one at $\Phi_{Me_2SO} = 0.45$ and 15 °C for which curvature in the angular dependence of the data persisted into the high-angle region. The lines and intercept from which M_w, A_2', and $\langle s^2\rangle_z$ were evaluated are shown. The relatively large

Table I
Experimental Results

Φ_{Me_2SO}		[η], mL/g	$(\partial n/\partial c_2)_\mu$, mL/g	$(\partial n/\partial c_2)_\mu$*, mL/g	$(\partial n/\partial c_2)_\mu$*/ $(\partial n/\partial c_2)_\mu$	$M_w \times 10^{-5}$, g/mol	$A_2' \times 10^5$, (mL mol)/g²	$\langle s^2\rangle_z^{1/2}$, Å	M_w* $\times 10^{-5}$, g/mol	A_2'* $\times 10^5$, (mL mol)/g²
0.30		65.7 ± 0.3	0.127 ± 0.003	0.127 ± 0.005	1.00	5.06 ± 0.38	5.56 ± 0.36	263 ± 14	5.06 ± 0.54	5.56 ± 0.54
0.35		70.5 ± 0.4	0.128 ± 0.005	0.122 ± 0.004	0.91	4.67 ± 0.53	6.70 ± 0.69	241 ± 12	5.14 ± 0.55	6.08 ± 0.59
0.39		71.9 ± 0.4	0.111 ± 0.004	0.118 ± 0.004	1.13	6.21 ± 0.66	7.42 ± 0.72	260 ± 14	5.50 ± 0.59	8.38 ± 0.81
0.43		74.2 ± 0.4	0.104 ± 0.005	0.113 ± 0.004	1.18	6.60 ± 0.86	7.84 ± 0.95	291 ± 15	5.59 ± 0.60	9.26 ± 0.90
0.45	15 °C	68.4 ± 0.3	0.119			7.06	12.0	384 ± 20		
	25 °C	79.0 ± 0.4	0.108 ± 0.003	0.110 ± 0.004	1.04	7.24 ± 0.59	7.42 ± 0.53	324 ± 17	6.98 ± 0.75	7.69 ± 0.75
	35 °C	85.0 ± 0.4	0.118			5.68	15.9	332 ± 17		
	45 °C	94.2 ± 0.5	0.147			4.06	33.6	344 ± 18		
0.47		79.2 ± 0.4	0.114 ± 0.004	0.108 ± 0.004	0.90	5.34 ± 0.56	10.5 ± 1.0	301 ± 16	5.95 ± 0.64	9.43 ± 0.91
0.50		83.4 ± 0.4	0.112 ± 0.003	0.105 ± 0.004	0.88	5.55 ± 0.44	12.3 ± 0.9	340 ± 18	6.31 ± 0.68	10.8 ± 1.0
0.60		96.1 ± 0.5	0.093 ± 0.006	0.093 ± 0.003	1.00	5.46 ± 0.89	17.4 ± 2.7	345 ± 18	5.46 ± 0.58	17.4 ± 1.7
0.70		115.0 ± 0.6	0.080 ± 0.003	0.082 ± 0.003	1.05	6.26 ± 0.61	20.2 ± 1.8	341 ± 18	5.96 ± 0.64	21.2 ± 2.1
0.80		143.0 ± 0.7	0.076 ± 0.003	0.075 ± 0.003	0.97	6.60 ± 0.67	27.6 ± 2.5	388 ± 20	6.78 ± 0.73	26.9 ± 2.6
0.90		157.0 ± 0.8	0.062 ± 0.008	0.070 ± 0.003	1.28	7.64 ± 2.24	27.2 ± 7.7	375 ± 20	5.99 ± 0.64	34.7 ± 3.4

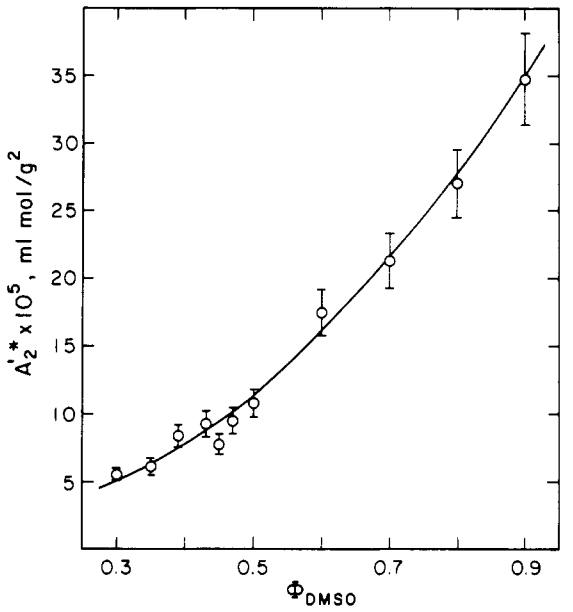

Figure 6. A plot vs. Φ_{Me_2SO} of the light-scattering second virial coefficient of amylose, $A_2'^*$, measured at 25 °C and based on the smoothed refractive increment, $(\partial n/\partial c_2)_\mu^*$.

standard deviation in $\bar{M}_w$ and $\bar{M}_w^*$ is occasioned in part by the long extrapolation from the high-angle data. Figures 5 and 6 show, respectively, the dependence of $\langle s^2\rangle_z^{1/2}$ and $A_2'^*$ on solvent composition. Extrapolation of the smooth curve in Figure 6 to $\Phi_{Me_2SO} = 0$ and 1 yields limiting values of $A_2'^*$ in good agreement with the results of other workers for amylose in H_2O[3,11] and Me_2SO.[17,19]

Uncertainties reported for M_w, A_2', and $\langle s^2\rangle_z^{1/2}$ were assumed to arise exclusively from uncertainty in $(\partial n/\partial c_2)_\mu$, which enters M_w and A_2' as the square through the optical constant K, and uncertainty in measured excess scattering intensities $i(\theta)$. Thus, the vertical bars appearing in Figure 4 represent the estimated experimental uncertainties in $c_2/\alpha i(\theta)$. Consideration of reasonable alternatives to the best straight lines through these data then permits estimates of the uncertainties in the slopes and intercept from which the several parameters are evaluated. Uncertainty in the slope of the line at $\theta = 100°$ averaged ±2.5%, whereas mean uncertainties in the slope and intercept of the extrapolated line at $c_2 = 0$ were ±7.0 and ±3.5%, respectively. The respective mean contributions from uncertainty in $i(\theta)$ to the uncertainties in M_w, A_2', and $\langle s^2\rangle_z^{1/2}$ were therefore ±3.5, 2.5, and 5.3%. Reported uncertainties in these parameters were computed by using the mean contributions from uncertainty in $i(\theta)$ and the contributions from the individual uncertainties in the corresponding values of $(\partial n/\partial c_2)_\mu$. Because of the apparent systematic errors in $(\partial n/\partial c_2)_\mu$ at temperatures different from 25 °C, no experimental uncertainties were attached to the corresponding values of M_w and A_2'. Attributing to every $(\partial n/\partial c_2)_\mu^*$ an uncertainty equal to the mean deviation of $(\partial n/\partial c_2)_\mu$ from the smoothed curve (±3.6%) and by using the mean contributions from uncertainty in $i(\theta)$, we report for all the uncertainties in M_w^* and $A_2'^*$, respectively, ±10.7 and 9.7%.

Unperturbed Dimensions

The unperturbed dimensions of a polymer dissolved in a moderately good solvent can be estimated from the measured dimensions in the good solvent, provided the molecular weight and the second virial coefficient are also known.[51-53] For polymer samples heterogeneous with respect to molecular weight, such as the unfractionated NRRC 5658:21 used in this work, it is necessary to have

information on the molecular weight distribution (MWD). Size exclusion chromatography studies of NRRC 5658:21 were carried out in this laboratory[54] by using H_2O/Me_2SO (Φ_{Me_2SO} = 0.50) as solvent with two serially connected columns each 2 ft long by 0.18 in. i.d. and packed with an equal pore volume mixture of 200/400 mesh controlled pore glass (Electro-Nucleonics, Fairfield, N.J.) with pore sizes 348 and 1060 Å. The columns were calibrated with essentially monodisperse[55] amylose samples synthesized from glucose 1-phosphate by using potato phosphorylase.[54] These studies indicate that the MWD of NRRC 5658:21 can be approximated satisfactorily by the Schulz–Flory distribution[56] characterized by M_n:M_w:M_z = 1:2:3, where M_n and M_z are, respectively, the number and z-average molecular weights, which may consequently be estimated from the measured M_w.

Polymer chain dimensions in H_2O/Me_2SO mixtures were obtained in the present studies directly as $\langle s^2\rangle_z$ from light scattering with eq 1 and by using the Flory–Fox relation[57] in eq 2, which relates the chain dimensions to the intrinsic

$$[\eta] = 6^{3/2}\Phi(\langle s^2\rangle_0/M)^{3/2}M_v^{1/2}\alpha^3 \quad (2)$$

viscosity through the viscosity parameter Φ.[51] The expansion factor $\alpha \equiv (\langle s^2\rangle/\langle s^2\rangle_0)^{1/2}$ measures the departure of $\langle s^2\rangle$ from the unperturbed value $\langle s^2\rangle_0$, M_v is the viscosity average molecular weight introduced in eq 2 to account for polymer heterogeneity and easily estimated from the measured M_w,[56,57] and $\langle s^2\rangle_0/M$ is a characteristic measure of the unperturbed homogeneous polymer coil dimensions which attains a limiting value for large molecular weight, M. This asymptotic behavior is reached for amylose at chain lengths well below those characteristic of NRRC 5658:21.[5,14,54] Unperturbed dimensions are reported here in terms of the characteristic ratio C_∞ defined above. From light scattering then we evaluate C_∞' as

$$C_\infty' = 6(\langle s^2\rangle_z/M_z)(M_u/\alpha^2L^2) \quad (3)$$

where M_u is the molecular weight of a glucose residue (162), the factor 6 interconverts $\langle s^2\rangle_0$ and $\langle r^2\rangle_0$,[57] and we assume following Berry and Casassa[53] that the ratio $\langle s^2\rangle_z/M_z$ for the heterogeneous sample closely approximates $\langle s^2\rangle/M$ for a homogeneous sample with $M = M_z$. From intrinsic viscosity we obtain C_∞'' by using eq 2 as

$$C_\infty'' = ([\eta]/\Phi M_v^{1/2})^{2/3}(M_u/\alpha^2L^2) \quad (4)$$

where the possible dependence of the product $\Phi M_v^{1/2}$ on solvent power (i.e., on α) is acknowledged.[51] It is assumed throughout that the small dependence of α on molecular weight[57] is negligible.

The observable parameter $\Psi \equiv (4\pi^{3/2}N)^{-1}A_2M^{1/2}(\langle s^2\rangle/M)^{-3/2}$ is a universal function of the expansion factor α for homogeneous polymer samples.[51-53] Here N is Avogadro's number, A_2 is the second virial coefficient, and the other parameters for the homogeneous polymer have already been defined. Several theories of the polymer excluded volume effect describe successfully the experimentally observed correlation of Ψ and α^3. The Yamakawa–Tanaka (YT) theory and the modified Flory–Krigbaum–Orofino (FKO) theory appear to be about equally satisfactory,[51] and their utility for polymers in mixed solvent systems has also been demonstrated.[52] In this work the modified FKO theory which relates α^2 and Ψ through eq 5 has been used.

$$\alpha^2 = 1 + 0.223[\exp(5.73\Psi) - 1] \quad (5)$$

We have evaluated Ψ for the heterogeneous NRRC 5658:21 in two ways. Using the light scattering results only we employ

$$\Psi' = (4\pi^{3/2}N)^{-1}A_2'M_w^{1/2}(\langle s^2\rangle_z/M_z)^{-3/2} \quad (6)$$

where $\langle s^2\rangle_z/M_z$ has been used to represent $\langle s^2\rangle/M$ as above, and we have replaced $A_2M^{1/2}$ by the quantity $A_2'M_w^{1/2}$ from light scattering as suggested by Berry and Casassa.[53] Alternatively, we replace $(\langle s^2\rangle/M)^{3/2}$ by $([\eta]/6^{3/2}\Phi M_v^{1/2})$ by using eq 2 to obtain

$$\Psi'' = (4\pi^{3/2}N)^{-1}A_2'M_w^{1/2}(6^{3/2}\Phi M_v^{1/2}/[\eta]) \quad (7)$$

Values of α^2 computed from eq 5 by using eq 6 and 7 will be denoted, respectively, $\alpha^2(\Psi')$ and $\alpha^2(\Psi'')$.

Whereas A_2', $\langle s^2\rangle_z$, and $[\eta]$ are expected to be strong functions of α, both Φ[52] and M_v[57] may also vary somewhat with α, and this circumstance needs to be recognized in the application of eq 4 and 7. (On the other hand, we do not expect Φ to be a function of M for the species present in NRRC 5658:21.[51,53,54]) It is reasonable to assume that the Mark–Houwink coefficient a for amylose is confined to the range 0.5–0.8 for the values of α encountered in the present mixed solvents.[3,24,57] Hence, the ratio $(M_v/M_w)^{1/2}$ is expected to increase by 4% from 0.94 to 0.98 for the Schulz–Flory MWD[56,57] as α increases through the observed range. A corresponding decline in Φ with increasing α of up to 8% is possible, if the behavior of polystyrene in mixed and single solvents can be taken as a guide.[52] Compensating changes in Φ and $M_v^{1/2}$ are therefore anticipated as α varies, and we assume in using eq 4 and 7 that the product $\Phi M_v^{1/2}$ is independent of α with $M_v^{1/2}$ = $0.94M_w^{1/2}$ and $\Phi = 2.2 \times 10^{23}$ mol^{-1}, a value consonant with the best experimental determinations of Φ for non-ionic polymers in good solvents.[58,59] (The consequences for C_∞ if the assumption of constant $\Phi M_v^{1/2}$ is wrong will be discussed below.)

It should be noted that the measurable quantities enter eq 7 as $A_2'M_w/[\eta]$. The product $A_2'M_w = A_2'^*M_w^*$ is completely independent of the relatively uncertain refractive increment (see eq 1), while $[\eta]$ is the most precisely known experimental quantity. Hence Ψ'' will have considerably greater precision than Ψ' (eq 6), which cannot be expressed in terms of quantities independent of the refractive increment and which depends in addition on the relatively uncertain mean square radius of gyration. All of the light-scattering results can be smoothed substantially, however, by using the smoothed refractive increment $(\partial n/\partial c_2)_\mu^*$ and the derived quantities M_w^* and $A_2'^*$ with $M_z = {}^3/_2M_w^*$. It is not advantageous in treating the light-scattering data to use the averaged molecular weight $\bar{M}_w^*$, because the respective experimental errors in $\langle s^2\rangle_z$ and M_w^* determined in a given light-scattering measurement tend to be compensating in the important ratio $\langle s^2\rangle_z/M_z$. On the other hand, it does seem appropriate in computing C_∞'' from eq 4 to replace $M_v^{1/2}$ by 0.94 $(\bar{M}_w^*)^{1/2}$, since measurements of $[\eta]$ and M_v are not coupled in the way that measurements of $\langle s^2\rangle_z$ and M_w^* are; the numerical factor 0.94 is explained above.

Values of Ψ' and Ψ'', obtained as described from eq 6 and 7, are given, respectively, in columns 2 and 3 of Table II and plotted in Figure 7, where the smooth curve is drawn to provide the best fit to the solvent dependence of Ψ''. It was not considered meaningful to evaluate Ψ' as a function of temperature at Φ_{Me_2SO} = 0.45, but the computed temperature dependence of Ψ'' in this solvent mixture is shown in Table II for the temperature range 25–45 °C. Table II presents in columns 4 and 5, respectively, the values of $\alpha^2(\Psi')$ and $\alpha^2(\Psi'')$ obtained with eq 5. The quantities Ψ' and $\alpha^2(\Psi')$ were not employed in further calculations because of the scatter, relative to Ψ'' and $\alpha^2(\Psi'')$, in their dependence on mixed solvent composition. We believe, however, that the results in Figure 7 confirm the essential equivalence of Ψ' and Ψ''. This evidence for the consistency of our light-scattering and viscometry data

Table II
Expansion Factors and Unperturbed Dimensions

Φ_{Me_2SO}		Ψ'	Ψ''	$\alpha^2(\psi')$	$\alpha^2(\psi'')$	$\Phi \times 10^{-23}$, mol^{-1}	C_∞'	C_∞''
0.30		0.107	0.0971 ± 0.003	1.189	1.166 ± 0.007	2.25	4.21	4.28 ± 0.16
0.35		0.157	0.101 ± 0.003	1.325	1.175 ± 0.007	3.22	3.45	4.45 ± 0.17
0.39		0.198	0.145 ± 0.004	1.470	1.289 ± 0.012	2.89	3.42	4.11 ± 0.16
0.43		0.161	0.158 ± 0.005	1.338	1.328 ± 0.016	2.18	4.09	4.07 ± 0.16
0.45	25 °C	0.151	0.154 ± 0.005	1.307	1.316 ± 0.015	2.35	4.10	4.28 ± 0.17
	35 °C		0.241 ± 0.007		1.664 ± 0.036			3.56 ± 0.15
	45 °C		0.328 ± 0.010		2.238 ± 0.084			2.83 ± 0.15
0.47		0.168	0.160 ± 0.005	1.361	1.335 ± 0.016	2.31	4.09	4.23 ± 0.16
0.50		0.150	0.186 ± 0.006	1.304	1.424 ± 0.022	1.84	4.62	4.10 ± 0.16
0.60		0.173	0.224 ± 0.007	1.378	1.582 ± 0.032	1.64	4.94	4.06 ± 0.17
0.70		0.260	0.249 ± 0.007	1.766	1.706 ± 0.037	2.31	4.10	4.24 ± 0.18
0.80		0.290	0.289 ± 0.009	1.952	1.945 ± 0.060	2.37	4.10	4.30 ± 0.21
0.90		0.323	0.300 ± 0.009	2.196	2.021 ± 0.064	2.39	4.17	4.40 ± 0.21

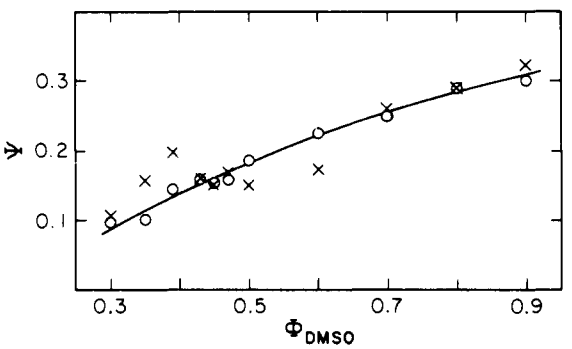

Figure 7. The quantity Ψ for amylose as a function of Φ_{Me_2SO} at 25 °C. Crosses refer to Ψ' from eq 6 and circles to Ψ'' from eq 7.

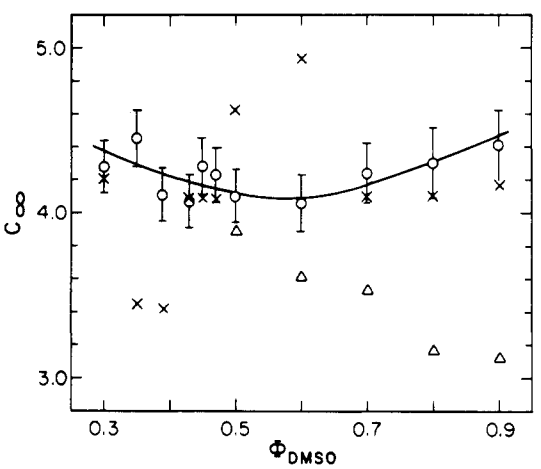

Figure 8. The characteristic ratio C_∞ of amylose as a function of Φ_{Me_2SO} at 25 °C. Crosses refer to C_∞' from eq 3, 5, and 7 and circles to C_∞'' from eq 4, 5, and 7. Triangles give C_∞ calculated from eq 4 and 7 by using the YT theory[51] in place of eq 5 (modified FKO theory) to evaluate α^2.

can be seen alternatively in the values of Φ calculated by using eq 2 (and the definition of α) from the measured values of $[\eta]$, $\langle s^2\rangle_z$, and M_w. The experimental quantity Φ given in column 6 of Table II was obtained by taking $\langle s^2\rangle/M = \langle s^2\rangle_z/M_z = \langle s^2\rangle_z/{}^3/_2M_w^*$ and $M_v^{1/2} = 0.94(\bar{M}^*)^{1/2}$. It shows no discernible trend with solvent composition, and its mean value (and standard deviation) is $(2.34 \pm 0.43) \times 10^{23}$ mol^{-1}, which agrees very well with the accepted value quoted above.

This agreement ensures that characteristic ratios C_∞'' from intrinsic viscosity data and eq 4, 5, and 7 will be in general agreement with the light-scattering dimensions C_∞' from eq 3, 5, and 7. Because the measurements of $[\eta]$ are much more precise than those of $\langle s^2\rangle_z$, the observed variation of C_∞'' with Φ_{Me_2SO} is certainly more reliable than that of C_∞'. The results are reported, respectively, in columns 8 and 7 of Table II and in Figure 8, where the smooth curve is drawn to fit the dependence of C_∞'' on solvent. Experimental uncertainties in C_∞'' average only about ±4.5%, a substantial part of which arises from the ±11% standard deviation in $\bar{M}_w^*$; smaller contributions come from the ±1–3% uncertainty in $\alpha^2(\Psi'')$ and the ±0.5% uncertainty in $[\eta]$. The quite satisfactory precision in C_∞'' derives primarily from the relative precision of $[\eta]$ but is also a consequence of the modest (±3.0%) uncertainty in Ψ'', which results from the high precision in measurements of $A_2'M_w$ (±2.5%) and $[\eta]$. Uncertainties in Ψ'' are barely perceptible on the scale of Figure 7 and were therefore omitted. No uncertainties were computed for the quantities Ψ', $\alpha^2(\Psi')$, and C_∞', which depend directly on the less precise refractive increment and/or light-scattering radius of gyration measurements.

Discussion

Results for C_∞'' presented in the previous section depend upon $A_2'M_w$ and $\bar{M}_w^*$ obtained by analyzing the light-scattering data with eq 1 and restricting attention to the high-angle ($100 \le \theta \le 150°$) region of the scattering envelope. Equation 1 is a standard result,[40,60,61] applicable in the range $30 \le \theta \le 150°$ provided $\langle s^2\rangle/(\lambda/n)^2$ is sufficiently small for all species present in the polymer sample.[62,63] When this condition is satisfied, the angular dependence of the extrapolated curve at $c_2 = 0$ in the Zimm plot (Figure 4) is expected to be linear for polymers with the Schulz–Flory MWD.[40] For larger $\langle s^2\rangle/(\lambda/n)^2$ the limiting behavior described by eq 1 may not be observable within the accessible range of θ.[63] Curvature in the $c_2 = 0$ line may also arise if the sample departs substantially from the Schulz–Flory MWD.[40] Negative curvature of the $c_2 = 0$ line at low angles only is often explained by the presence of a small weight fraction of material with molecular weights and dimensions much larger than those characterizing the bulk of the sample.[64,65] The occurrence of such particles in amylose[44,66] and other polysaccharides[45–47,67,68] has frequently been reported.

In analyzing the high-angle portion of the $c_2 = 0$ line with eq 1 we assume that the present amylose sample consists of a major component satisfying the above stated requirements on $\langle s^2\rangle/(\lambda/n)^2$ and MWD plus a minor component of significantly larger mass and chain dimensions which contributes perceptibly to the scattering only in the low-angle ($30 \le \theta \le 90°$) region. Since the postulated minor component is expected to have a negligible influence on $[\eta]$,[45,57] it is readily shown[69] by using eq 2 that the chain dimensions of the molecules constituting the major component of NRRC 5658:21 are sufficiently compact for all Φ_{Me_2SO} to render the limiting behavior in eq 1

applicable throughout the range $30 \leq \theta \leq 150°$. It is likewise shown[69] by using methods described recently[47] that the observed angular dependence of the present $c_2 = 0$ curves can be fully explained by postulating contamination of amylose chains having the characteristics reported in Table I by large ($\langle s^2 \rangle^{1/2} \geq 1000$ Å) spherical or branched chain particles with $M_w \simeq 10^8$ present in a proportion so small (<0.05% w/w) as to render negligible their contribution to $[\eta]$ and c_2. This material might be aggregated amylose and/or residual amylopectin and would not have been eliminated by the clarification procedures described above.

Evaluation of A_2' from the concentration dependence of $Kc_2/\alpha i(\theta)$ at $\theta = 100°$ is consistent with eq 1 derived by Zimm[39] in the "single contact approximation". More generally the term proportional to c_2 may also include an angle-dependent factor.[70,71] We justify our procedure for obtaining A_2' by the absence of any perceptible variation of the slope of the concentration dependence with angle for $\theta \geq 100°$. The consistent linearity of these curves militates against interpreting the extremely large component of our amylose sample as a rapidly equilibrating aggregation product of amylose.[47,65] The agreement within experimental error shown in Figures 7 and 8 of the respective quantities Ψ' and C_∞' from light scattering with the viscometrically determined Ψ'' and C_∞'' provides substantial support for the methods employed to treat the experimental data. In particular, the assumption of constant $\Phi M_v^{1/2}$ in eq 4 and 7 is not called into question. Had $\Phi M_v^{1/2}$ been assumed to decline with increasing Φ_{Me_2SO} (increasing α), the effect would have been to increase the values of C_∞'' corresponding to larger Φ_{Me_2SO} relative to those at low Φ_{Me_2SO}. The light-scattering results C_∞' do not show this tendency and are thus consistent with the assumption that $\Phi M_v^{1/2}$ is constant.

The most serious question about the reliability of the reported solvent dependence of C_∞'' involves the choice of theory for computing α^2 from the observable Ψ''. We have chosen to use the modified FKO theory because it appears to provide a marginally better correlation of existing experimental plots[51] of Ψ vs. α^3 throughout most of the experimental range. However, for larger values of Ψ (i.e., $\Psi > \sim 0.25$) the YT theory may provide the better correlation.[51,52] Plots of Ψ vs. α^3 from the two theories begin to diverge near $\Psi = 0.150$ with the YT theory approaching a smaller asymptotic value of Ψ at large α^3 than the modified FKO theory.[51] Consequently α^2 values calculated from measured Ψ values will be larger with the use of the YT theory. This difference begins to exceed the experimental uncertainty of our data for $\Psi \geq 0.170$, and we have therefore computed C_∞'' from eq 4 and 7 with $\alpha^2(\Psi'')$ from the YT theory for $\Phi_{Me_2SO} \geq 0.50$. These values of C_∞'' are plotted as triangles in Figure 8.

Regardless of which theory is employed to compute α^2 in the Me_2SO-rich solvent mixtures, it appears that the characteristic ratio C_∞'' has a value near $\Phi_{Me_2SO} = 0.50$ some 20% smaller than the accepted characteristic ratio (~ 5) of aqueous amylose. Cowie has suggested that the unperturbed dimensions at $\Phi_{Me_2SO} = 0.25$ are also smaller than those in 0.5 M aqueous KCl.[24] A plausible extrapolation of the curve in Figure 8 can be drawn to an ordinate intercept near 5 at $\Phi_{Me_2SO} = 0$, and we are inclined to believe that the plot of C_∞ vs. Φ_{Me_2SO} in fact displays a monotonic decline out to about $\Phi_{Me_2SO} = 0.60$. The behavior of C_∞ at still larger Φ_{Me_2SO} remains uncertain and must await a definitive procedure for evaluating α^2 from relatively large values of Ψ. A temperature coefficient $\partial \ln C_\infty''/\partial T = -0.02$ deg^{-1} can be evaluated from data in the range 25–45 °C for $\Phi_{Me_2SO} = 0.45$. This unusually large[72,73] negative value is consistent in sign with earlier results[14] for aqueous amylosic chains. The negative sign presumably finds an explanation at the molecular level similar to that advanced earlier for aqueous amylose.[2,5,7] Note that a still more negative, and less plausible, temperature coefficient would arise from use of the YT theory to evaluate α^2.

It is interesting to contrast the negative temperature coefficient of C_∞'' with the strongly positive value of $\partial \ln [\eta]/\partial T$ (0.01 deg^{-1}) observed in the same solvent mixture; the mixture with $\Phi_{Me_2SO} = 0.45$ evidently becomes a better solvent for amylose as the temperature increases. In the pure solvents H_2O and Me_2SO the respective intrinsic viscosities $[\eta]_{H_2O}$ and $[\eta]_{Me_2SO}$ both decrease with increasing temperature,[14] so that the quantity $\Delta[\eta]$ defined by

$$\Delta[\eta] \equiv [\eta] - \{\Phi_{Me_2SO}[\eta]_{Me_2SO} + (1 - \Phi_{Me_2SO})[\eta]_{H_2O}\} \quad (8)$$

becomes less negative with increasing T as predicted in the first approximation by polymer solution theory[25] for polymers dissolved in binary solvents like H_2O/Me_2SO formed with a negative heat of mixing. The dependence of $[\eta]$ on Φ_{Me_2SO} resembles qualitatively that reported by Cowie,[24] although there is a discrepancy in the magnitude of $[\eta]$ when a comparison is made with Cowie's fraction BF6 for which the reported M_w is the same as that of NRRC 5658:21. This discrepancy is unlikely to be a consequence of differences in MWD,[69] and there is in fact reason to believe that Cowie's reported molecular weights may be too high.[3,19] The unusual inflection point in the plot of $[\eta]$ vs. Φ_{Me_2SO} mentioned earlier as well as an inflection in the plot of $(\partial n/\partial c_2)_\mu$ occur near $\Phi_{Me_2SO} = 0.66$, where the stoichiometry of the 2:1 (H_2O:Me_2SO) complex is satisfied and the identity of the preferentially solvating species changes.[31] There is otherwise nothing in the results reported here to suggest any peculiarities in the system associated with this binary solvent composition.

Dondos and Benoit[26] have argued that because preferential solvation in mixed solvents renders the local solvent composition within a polymer coil different from the composition of the solvent intervening between polymer coils, the mean interaction between two segments of the same polymer chain may differ from that between two segments of separate polymer chains. To the extent that this is true the expansion factor α could differ from unity under conditions where the second virial coefficient vanishes, and the validity of relationships between A_2' and α^2, e.g., eq 5, is called into question. Experimental investigations of the correlation of Ψ and α^3 in mixed solvents[52] yield results which accord very well with those in two-component systems,[51] especially in mixed solvents approaching the Θ condition for which Dondos and Benoit[26] expect the effect of differing inter- and intramolecular excluded volume effects to be most pronounced. These same authors have reported an empirical correlation of polymer unperturbed dimensions in mixed binary solvents with the excess free energy of mixing of the binary solvent mixture.[74,75] Applied to the present system the correlation supports the occurrence of a minimum in the C_∞'' vs. Φ_{Me_2SO} plot (Figure 8), since the excess free energy clearly must display a minimum.

In conclusion we believe it is demonstrated that specific solvation effects cause the unperturbed dimensions of amylose to decline by perhaps 20% as the composition of the mixed solvent H_2O/Me_2SO varies from $\Phi_{Me_2SO} = 0$ to 0.60. Reduction in C_∞ is consistent with a shift in the domain of preferred maltose conformers from the region of left helix chirality near the point X in Figure 1 in the direction of increasing ϕ and ψ. As explained elsewhere,[2,5,7]

a preference for conformers, which if repeated in sequence produce helices of low pitch, leads also to random coils with small unperturbed dimensions. Independent evidence for induction by Me_2SO of just this sort of shift in preferred ϕ and ψ values has been reviewed in the introduction. Further changes in C_∞ for $\Phi_{Me_2SO} > 0.60$ cannot be ascertained with confidence at the present time. Other studies discussed above suggest rather convincingly, however, that intramolecular hydrogen bonding is a characteristic feature of amylose in Me_2SO solution.[20,21] If so, the energy map of Figure 1, which includes no hydrogen-bonded interactions,[5,33] must inevitably change in the direction of greater conformational constraint, increased tendency of the chain toward helical propagation, and larger characteristic ratio. To the extent that intramolecular hydrogen bonding is encouraged in Me_2SO, the possible role of longer range interactions in determining C_∞ must be acknowledged and the adequacy of a simple maltose map (Figure 1) to provide a full description of the properties of the unperturbed chain questioned.

Acknowledgment. This work has been supported by NSF Research Grants PCM77-23603 and BMS73-08595A02.

References and Notes

(1) D. A. Rees, *MPT Int. Rev. Sci.: Org. Chem., Ser. One*, 7, 251 (1973).
(2) D. A. Brant in "The Biochemistry of Plants", Vol. 3, J. Preiss, Ed., Academic Press, New York, in press.
(3) W. Banks and C. T. Greenwood, "Starch and Its Components", Edinburgh University Press, Edinburgh, 1975.
(4) V. S. R. Rao, N. Yathindra, and P. R. Sundararajan, *Biopolymers*, 8, 325 (1969).
(5) D. A. Brant and W. L. Dimpfl, *Macromolecules*, 3, 655 (1970).
(6) R. C. Jordan, D. A. Brant, and A. Cesàro, *Biopolymers*, 17, 2617 (1978).
(7) D. A. Brant, *Q. Rev. Biophys.*, 9, 527 (1976).
(8) C. V. Goebel, W. L. Dimpfl, and D. A. Brant, *Macromolecules*, 3, 644 (1970).
(9) E. Husemann, B. Pfannemueller, and W. Burchard, *Makromol. Chem.*, 59, 1 (1963).
(10) W. Burchard, *Makromol. Chem.*, 59, 16 (1963).
(11) W. Burchard, *Makromol. Chem.*, 64, 110 (1963).
(12) B. Pfannemueller, H. Mayerhoefer, and R. C. Schulz, *Biopolymers*, 10, 243 (1971).
(13) M. Kodama, H. Noda, and T. Kamata, *Biopolymers*, 17, 985 (1978).
(14) K. D. Goebel and D. A. Brant, *Macromolecules*, 3, 634 (1970).
(15) W. W. Everett and J. F. Foster, *J. Am. Chem. Soc.*, 81, 3459 (1959).
(16) W. W. Everett and J. F. Foster, *J. Am. Chem. Soc.*, 81, 3464 (1959).
(17) J. M. G. Cowie, *Makromol. Chem.*, 42, 230 (1961).
(18) J. M. G. Cowie, *Makromol. Chem.*, 53, 13 (1962).
(19) M. Fujii, K. Honda, and H. Fujita, *Biopolymers*, 12, 1177 (1973).
(20) B. Casu, M. Reggiani, G. G. Gallo, and A. Vigevani, *Tetrahedron*, 22, 3061 (1966).
(21) M. St. Jacques, P. R. Sundararajan, K. J. Taylor, and R. H. Marchessault, *J. Am. Chem. Soc.*, 98, 4386 (1976).
(22) D. A. Rees and P. J. C. Smith, *J. Chem. Soc., Perkin Trans. 2*, 836 (1975).
(23) D. A. Rees and D. Thom, *J. Chem. Soc., Perkin Trans. 2*, 191 (1977).
(24) J. M. G. Cowie, *Makromol. Chem.*, 59, 189 (1963).
(25) J. Pouchlý and D. Patterson, *Macromolecules*, 9, 574 (1976).
(26) A. Dondos and H. Benoit in "Order in Polymer Solutions", K. Šolc, Ed., Gordon and Breach, New York, 1973, p 175.
(27) A. Dondos and D. Patterson, *J. Polym. Sci., Part A-2*, 7, 209 (1969).
(28) F. R. Dintzis and R. Tobin, *Biopolymers*, 7, 581 (1969).
(29) I. Bulla, P. Törmälä, and J. J. Lindberg, *Acta Chem. Scand., Ser. A*, 29, 89 (1975).
(30) H. Kelm, J. Klosowski, and E. Steger, *J. Mol. Struct.*, 28, 1 (1975).
(31) P. R. Straub and D. A. Brant, *Biopolymers*, 19, 639 (1980).
(32) A. Heyraud, M. Rinaudo, M. Vignon, and M. Vincendon, *Biopolymers*, 18, 167 (1979).
(33) D. A. Brant and K. D. Goebel, *Macromolecules*, 8, 522 (1975).
(34) T. J. Schoch, *Adv. Carbohydr. Chem.*, 1, 274 (1945).
(35) E. F. Casassa and H. Eisenberg, *Adv. Protein Chem.*, 19, 287 (1964).
(36) W. B. Dandliker and J. Kraut, *J. Am. Chem. Soc.*, 78, 2380 (1956).
(37) D. J. Coumou, *J. Colloid Sci.*, 15, 408 (1960).
(38) G. Cohen and H. Eisenberg, *J. Chem. Phys.*, 43, 3881 (1965).
(39) B. H. Zimm, *J. Chem. Phys.*, 16, 1093 (1948).
(40) B. H. Zimm, *J. Chem. Phys.*, 16, 1099 (1948).
(41) J. M. G. Cowie and P. M. Toporowski, *Can. J. Chem.*, 39, 2240 (1961).
(42) R. G. LeBel and D. A. I. Goring, *J. Chem. Eng. Data*, 7, 100 (1962).
(43) R. van Wijk and A. J. Staverman, *J. Polym. Sci., Part A-2*, 4, 1011 (1966).
(44) F. R. Dintzis and R. Tobin, *Carbohydr. Res.*, 66, 71 (1978).
(45) D. W. Tanner and G. C. Berry, *J. Polym. Sci., Polym. Phys. Ed.*, 12, 941 (1974).
(46) C. Holt, W. Mackie, and D. B. Sellen, *Polymer*, 17, 1027 (1976).
(47) R. C. Jordan and D. A. Brant, *Biopolymers*, 17, 2885 (1978).
(48) M. R. Cannon, R. E. Manning, and J. D. Bell, *Anal. Chem.*, 32, 355 (1960).
(49) M. B. Huglin in "Light Scattering from Polymer Solutions", M. B. Huglin, Ed., Academic Press, New York, 1972, p 165.
(50) W. Banks and C. T. Greenwood, *Makromol. Chem.*, 67, 49 (1963).
(51) H. Yamakawa, "Modern Theory of Polymer Solutions", Harper and Row, New York, 1971.
(52) K. Takashima, K. Nakae, M. Shibata, and H. Yamakawa, *Macromolecules*, 7, 641 (1974).
(53) G. C. Berry and E. F. Casassa, *J. Polym. Sci., Macromol. Rev.*, 4, 1 (1970).
(54) P. R. Straub, M.S. Thesis, University of California, Irvine, 1978.
(55) B. Pfannemueller and W. Burchard, *Makromol. Chem.*, 121, 1 (1969).
(56) L. H. Peebles, Jr., "Molecular Weight Distributions in Polymers", Wiley-Interscience, New York, 1971.
(57) P. J. Flory, "Principles of Polymer Chemistry", Cornell University Press, Ithaca, New York, 1953.
(58) S. Newman, W. R. Krigbaum, C. Laugier, and P. J. Flory, *J. Polym. Sci.*, 14, 451 (1954).
(59) W. R. Krigbaum and D. K. Carpenter, *J. Phys. Chem.*, 59, 1166 (1955).
(60) P. J. Flory and R. L. Jernigan, *J. Am. Chem. Soc.*, 90, 3128 (1968).
(61) T. E. Smith and D. K. Carpenter, *Macromolecules*, 1, 204 (1968).
(62) H. Benoit, *J. Polym. Sci.*, 11, 507 (1953).
(63) A. Holtzer, H. Benoit, and P. Doty, *J. Phys. Chem.*, 58, 624 (1954).
(64) P. Kratochvil in "Light Scattering from Polymer Solutions", M. B. Huglin, Ed., Academic Press, New York, 1972, p 333.
(65) H.-G. Elias in "Light Scattering from Polymer Solutions", M. B. Huglin, Ed., Academic Press, New York, 1972, p 397.
(66) W. Burchard and B. Pfannemueller, *Makromol. Chem.*, 121, 18 (1969).
(67) O. Smidsrød and A. Haug, *Acta Chem. Scand.*, 22, 797 (1968).
(68) M. M. Huque, D. A. I. Goring, and S. G. Mason, *Can. J. Chem.* 36, 952 (1958).
(69) R. C. Jordan, Ph.D. Dissertation, University of California, Irvine, 1976.
(70) P. J. Flory and A. M. Bueche, *J. Polym. Sci.*, 27, 219 (1958).
(71) D. B. Siano and J. Applequist, *Macromolecules*, 8, 858 (1975).
(72) P. J. Flory, "Statistical Mechanics of Chain Molecules", Wiley-Interscience, New York, 1969.
(73) S. Bluestone, J. E. Mark, and P. J. Flory, *Macromolecules*, 7, 325 (1974).
(74) A. Dondos and H. Benoit, *Macromolecules*, 4, 279 (1971).
(75) A. Dondos and H. Benoit, *Macromolecules*, 6, 242 (1973).